Prospects for measuring Higgs triscalar coupling at the HL-LHC and HL-100 TeV hadron collider

Chih-Ting Lu

(NTHU)

Collaborators : Prof. Kingman Cheung, Prof. Jae Sik Lee, Dr. Jubin Park, Dr. Jung Chang

Ref : **JHEP 1508 (2015) 133**

1804.07130

Contents

* 1. Motivations
* 2. Effective Lagrangian
* 3. Outline of simulations and event selections
* 4. Essence of analysis results at the HL-LHC and HL-100 TeV hadron collider
* 5. Conclusions

Motivations

- Self-coupling of the Higgs boson is a crucial property which depends on the dynamics of the EWSB sector.
- One of the probes of Higgs self-coupling is the Higgs-boson-pair production at the LHC.
- In this work, we perform the most up-to-date comprehensive signal-background analysis for Higgs-pair production through gluon fusion and the $HH \to b\bar{b}\gamma\gamma$ channel at the HL-LHC and HL-100 TeV hadron collider, with the goal of probing the self-coupling λ_{3H} of the Higgs boson.

Effective Lagranian

$$-\mathcal{L} = \frac{1}{3!}\left(\frac{3M_H^2}{v}\right)\lambda_{3H}\,H^3 \;+\; g_t^S\,\frac{m_t}{v}\,\bar{t}\,t\,H$$

In the SM, $\lambda_{3H} = g_t^S = 1$.

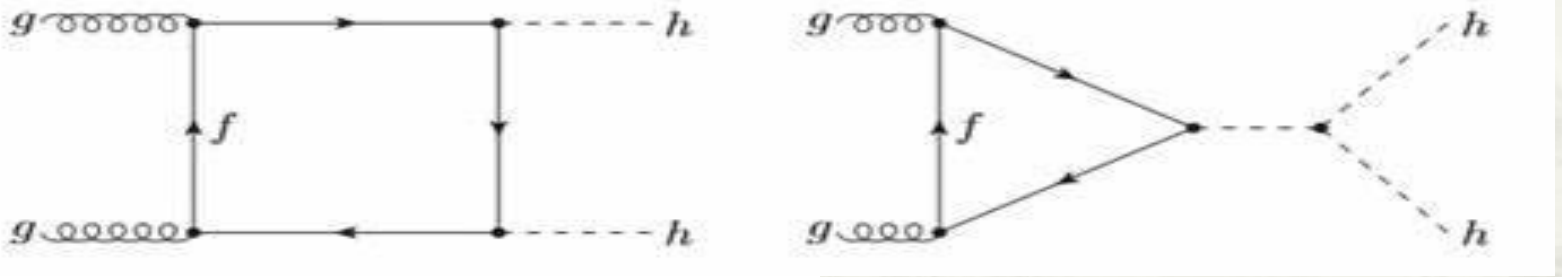

$$g(p_1)g(p_2) \;\rightarrow H(p_3)H(p_4)$$

$$\frac{d\hat{\sigma}(gg\rightarrow HH)}{d\hat{t}} = \frac{G_F^2\alpha_s^2}{512(2\pi)^3}\left[\left|\lambda_{3H}g_t^S D(\hat{s})F_\triangle^S + (g_t^S)^2F_\square^{SS}\right|^2 + \left|(g_t^S)^2G_\square^{SS}\right|^2\right]$$

Effective Lagranian

where

$$D(\hat{s}) = \frac{3M_H^2}{\hat{s} - M_H^2 + iM_H\Gamma_H}$$

and $\hat{s} = (p_1 + p_2)^2$, $\hat{t} = (p_1 - p_3)^2$, and $\hat{u} = (p_2 - p_3)^2$ with $p_1 + p_2 = p_3 + p_4$.

In the heavy quark limit, one may have

$$F_{\triangle}^{S} = +\frac{2}{3} + \mathcal{O}(\hat{s}/m_Q^2)\,, \quad F_{\square}^{SS} = -\frac{2}{3} + \mathcal{O}(\hat{s}/m_Q^2)\,, \quad G_{\square}^{SS} = \mathcal{O}(\hat{s}/m_Q^2)$$

leading to large cancellation between the triangle and box diagrams.

Effective Lagranian

The production cross section normalized to the corresponding SM cross section, with or without cuts, can be parameterized as follows:

$$\frac{\sigma^{\rm LO}(gg \to HH)}{\sigma^{\rm LO}_{\rm SM}(gg \to HH)} = c_1(s)\,\lambda_{3H}^2\,(g_t^S)^2 + c_2(s)\,\lambda_{3H}\,(g_t^S)^3 + c_3(s)\,(g_t^S)^4 \qquad (5)$$

where the numerical coefficients $c_{1,2,3}(s)$ depend on s and experimental selection cuts. Numerically, $c_1(s), c_2(s), c_3(s)$ are $0.263\,, -1.310\,, 2.047$ at 14 TeV and $0.208\,, -1.108\,, 1.900$ at 100 TeV [11]. Upon our normalization, the ratio should be equal to 1 when $g_t^S = \lambda_{3H} = 1$, or $c_1(s) + c_2(s) + c_3(s) = 1$. The coefficients $c_1(s)$ and $c_3(s)$ are for the contributions from the triangle and box diagrams, respectively, and the coefficient $c_2(s)$ for the interference between them. Once we have the coefficients c_i the cross sections can be easily obtained for any combinations of couplings.

Outline of simulations and event selections

* Our goal is to disentangle the effects of trilinear Higgs coupling, which is present in the triangle diagram, in Higgs-pair production.
* We vary the value for the trilinear coupling λ_{3H} between -5 and 10 to visualize the effects of λ_{3H} .
* The backgrounds include

- single-Higgs associated production, such as ggH, $t\bar{t}H$, ZH, $b\bar{b}H$ followed by $H \to \gamma\gamma$,
- non-resonant backgrounds and jet-fake backgrounds, such as $b\bar{b}\gamma\gamma$, $c\bar{c}\gamma\gamma$, $jj\gamma\gamma$, $b\bar{b}j\gamma$, $c\bar{c}j\gamma$, $b\bar{b}jj$, and $Z\gamma\gamma \to b\bar{b}\gamma\gamma$,
- $t\bar{t}(\geq 1$ lepton) and $t\bar{t}\gamma(\geq 1$ lepton) backgrounds .

Signal					
Signal process		Generator/Parton Shower	$\sigma \cdot BR$ [fb]	Order in QCD	PDF used
$gg \to HH \to b\bar{b}\gamma\gamma$ [15]		MG5_aMC@NLO/PYTHIA8	0.119	NNLO +NNLL	NNPDF2.3LO
Backgrounds					
Background(BG)	Process	Generator/Parton Shower	$\sigma \cdot BR$ [fb]	Order in QCD	PDF used
Single-Higgs associated BG [15]	$ggH(\to \gamma\gamma)$	POWHEG − BOX/PYTHIA6	1.20×10^2	NNNLO	CT10
	$t\bar{t}H(\to \gamma\gamma)$	PYTHIA8/PYTHIA8	1.37	NLO	
	$ZH(\to \gamma\gamma)$	PYTHIA8/PYTHIA8	2.24	NLO	
	$b\bar{b}H(\to \gamma\gamma)$	PYTHIA8/PYTHIA8	1.26	NLO	
Non-resonant BG	$b\bar{b}\gamma\gamma$	MG5_aMC@NLO/PYTHIA8	1.40×10^2	LO	CTEQ6L1
	$c\bar{c}\gamma\gamma$	MG5_aMC@NLO/PYTHIA8	1.14×10^3	LO	
	$jj\gamma\gamma$	MG5_aMC@NLO/PYTHIA8	1.62×10^4	LO	
	$b\bar{b}j\gamma$	MG5_aMC@NLO/PYTHIA8	3.67×10^5	LO	
	$c\bar{c}j\gamma$	MG5_aMC@NLO/PYTHIA8	1.05×10^6	LO	
	$b\bar{b}jj$	MG5_aMC@NLO/PYTHIA8	4.34×10^8	LO	
	$Z(\to b\bar{b})\gamma\gamma$	MG5_aMC@NLO/PYTHIA8	5.17	LO	
$t\bar{t}$ and $t\bar{t}\gamma$ BG (≥ 1 lepton)	$t\bar{t}$ [18]	POWHEG − BOX/PYTHIA8	5.30×10^5	NNLO +NNLL	CT10
	$t\bar{t}\gamma$ [19]	MG5_aMC@NLO/PYTHIA8	1.60×10^3	NLO	CTEQ6L1

LHC-14

TABLE III. The main fake processes and the corresponding rates in each sample of non-resonant and $t\bar{t}(\gamma)$ backgrounds. We recall that $P_{j\to\gamma} = 5\times10^{-4}$ and $P_{c\to\gamma} = 2\%/5\%$ in the barrel/endcap calorimeter region. For c_s quarks produced during showering in the $jj\gamma\gamma$ sample, we use $P_{c_s\to b} = 1/8$ as in Ref. [26]. Otherwise the P_T and η dependence of $P_{c\to b}$ is fully considered as explained in the text.

Background(BG)	Process	Fake Process	Fake rate
Non-resonant BG	$b\bar{b}\gamma\gamma$	N/A	N/A
	$c\bar{c}\gamma\gamma$	$c\to b,\ \bar{c}\to\bar{b}$	$(P_{c\to b})^2$
	$jj\gamma\gamma$	$c_s\to b,\ \bar{c_s}\to\bar{b}$	$(P_{c_s\to b})^2$
	$b\bar{b}j\gamma$	$j\to\gamma$	5×10^{-4}
	$c\bar{c}j\gamma$	$c\to b,\ \bar{c}\to\bar{b},\ j\to\gamma$	$(P_{c\to b})^2\cdot(5\times10^{-4})$
	$b\bar{b}jj$	$j\to\gamma,\ j\to\gamma$	$(5\times10^{-4})^2$
	$Z(\to b\bar{b})\gamma\gamma$	N/A	N/A
$t\bar{t}$	Leptonic decay	$e\to\gamma,\ e\to\gamma$	$(0.02)^2/0.02\cdot0.05/(0.05)^2$
	Semi-leptonic decay	$e\to\gamma,\ j\to\gamma$	$(0.02)\cdot5\times10^{-4}/(0.05)\cdot5\times10^{-4}$
$t\bar{t}\gamma$	Leptonic decay	$e\to\gamma$	0.02/0.05
	Semi-leptonic	$e\to\gamma$	0.02/0.05

Outline of simulations and event selections

TABLE IV. Sequence of event selection criteria at the HL-LHC applied in this analysis.

Sequence	Event Selection Criteria at the HL-LHC
1	Di-photon trigger condition, ≥ 2 isolated photons with $P_T > 25$ GeV, $\|\eta\| < 2.5$
2	≥ 2 isolated photons with $P_T > 30$ GeV, $\|\eta\| < 1.37$ or $1.52 < \|\eta\| < 2.37$, $\Delta R_{j\gamma} > 0.4$
3	≥ 2 jets identified as b-jets with leading(subleading) $P_T > 40(30)$ GeV, $\|\eta\| < 2.4$
4	Events are required to contain ≤ 5 jets with $P_T > 30$ GeV within $\|\eta\| < 2.5$
5	No isolated leptons with $P_T > 25$ GeV, $\|\eta\| < 2.5$
6	$0.4 < \Delta R_{b\bar{b}} < 2.0$, $0.4 < \Delta R_{\gamma\gamma} < 2.0$
7	$122 < M_{\gamma\gamma}/\text{GeV} < 128$ and $100 < M_{b\bar{b}}/\text{GeV} < 150$
8	$P_T^{\gamma\gamma} > 80$ GeV, $P_T^{b\bar{b}} > 80$ GeV

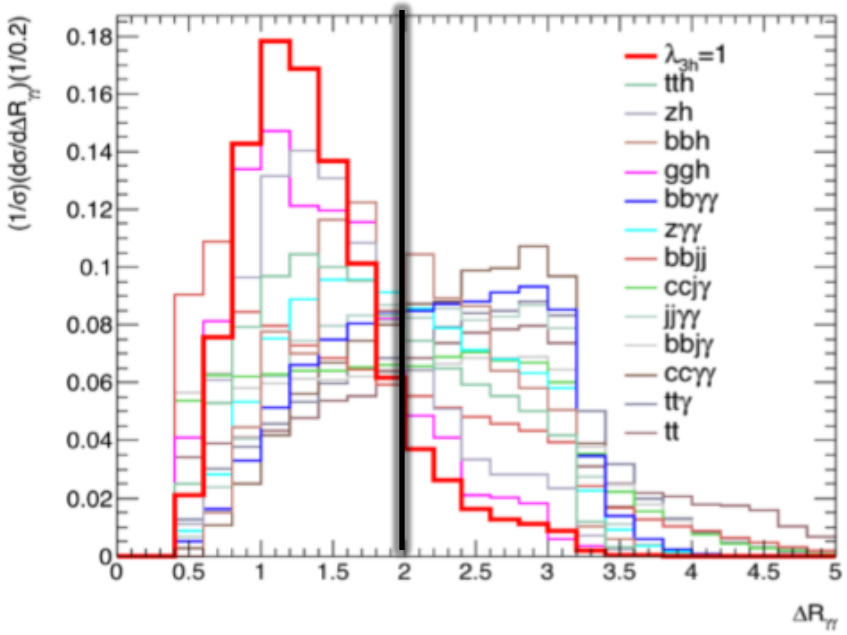
$(1/\sigma)(d\sigma/d\Delta R_{\gamma\gamma})(1/0.2)$
λ_{3h}=1
tth
zh
bbh
ggh
bbγγ
zγγ
bbjj
ccjγ
jjγγ
bbjγ
ccγγ
ttγ
tt
$\Delta R_{\gamma\gamma}$

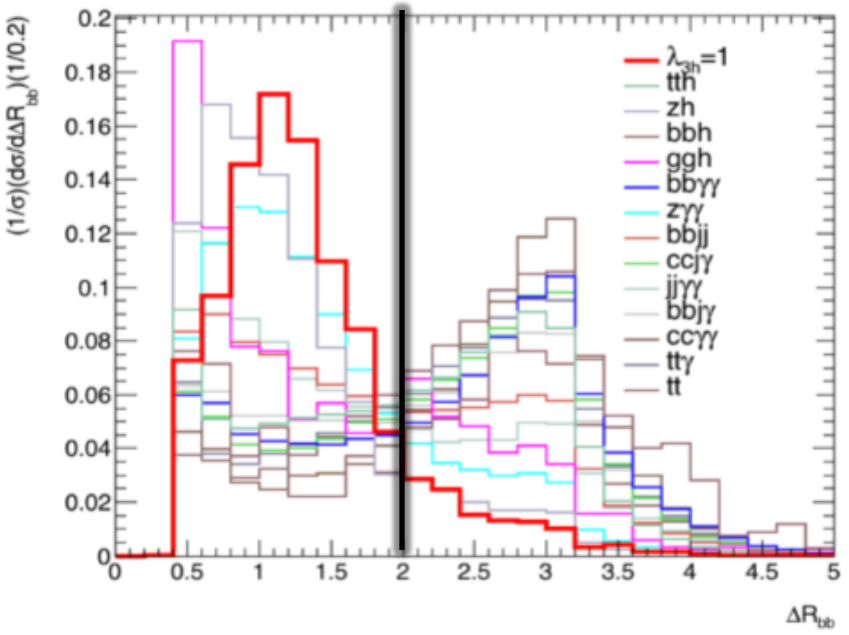
$(1/\sigma)(d\sigma/d\Delta R_{bb})(1/0.2)$
λ_{3h}=1
tth
zh
bbh
ggh
bbγγ
zγγ
bbjj
ccjγ
jjγγ
bbjγ
ccγγ
ttγ
tt
ΔR_{bb}

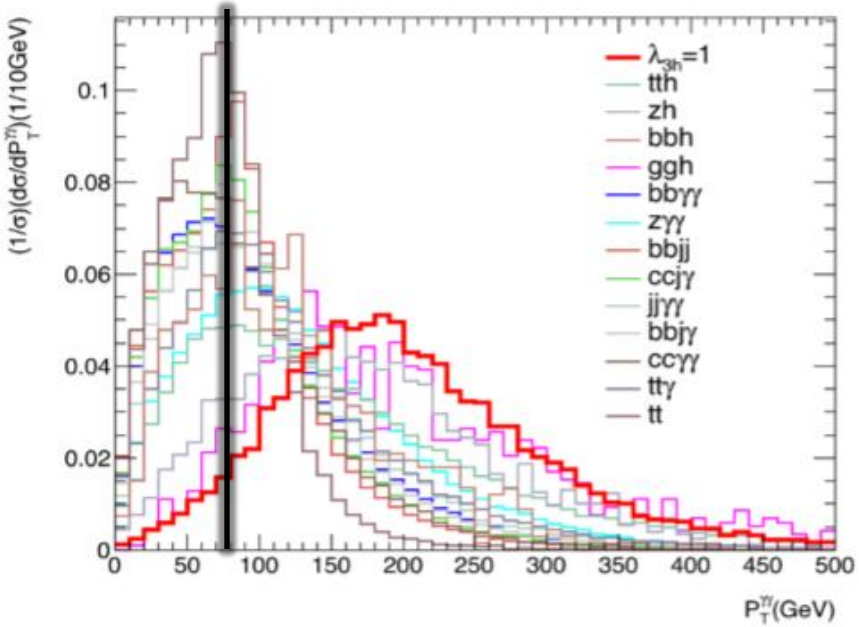
$(1/\sigma)(d\sigma/dP_T^{\gamma\gamma})(1/10GeV)$
λ_{3h}=1
tth
zh
bbh
ggh
bbγγ
zγγ
bbjj
ccjγ
jjγγ
bbjγ
ccγγ
ttγ
tt
$P_T^{\gamma\gamma}$(GeV)

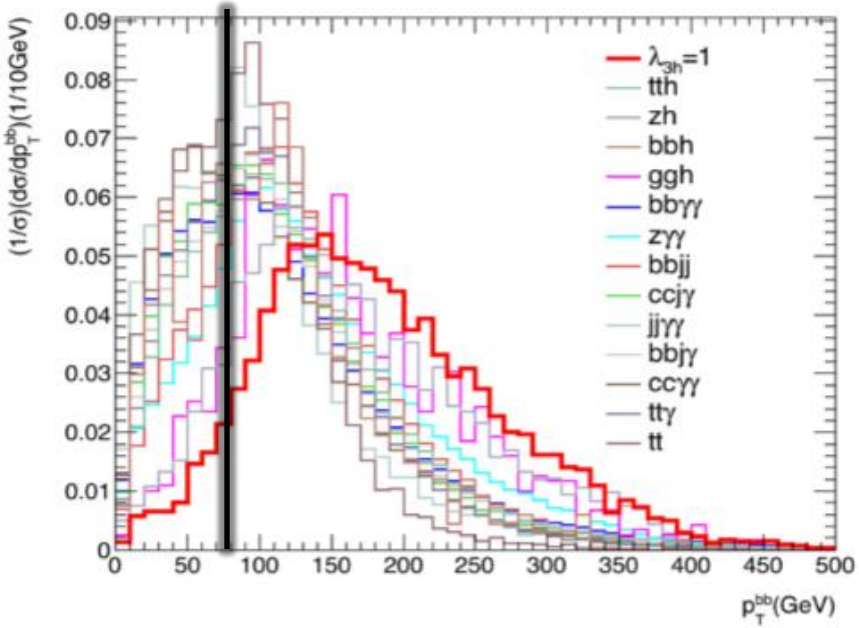
$(1/\sigma)(d\sigma/dp_T^{bb})(1/10GeV)$
λ_{3h}=1
tth
zh
bbh
ggh
bbγγ
zγγ
bbjj
ccjγ
jjγγ
bbjγ
ccγγ
ttγ
tt
p_T^{bb}(GeV)

Expected yields (3000 fb^{-1}) Samples	Total	Barrel-barrel	Other (End-cap)	Ratio (O/B)
$H(b\bar{b})\,H(\gamma\gamma)$, $\lambda_{3H}=-4$	77.14	57.03	20.11	0.35
$H(b\bar{b})\,H(\gamma\gamma)$, $\lambda_{3H}=0$	19.50	14.33	5.17	0.36
$H(b\bar{b})\,H(\gamma\gamma)$, $\lambda_{3H}=1$	11.42	8.53	2.89	0.34
$H(b\bar{b})\,H(\gamma\gamma)$, $\lambda_{3H}=2$	6.82	5.14	1.68	0.33
$H(b\bar{b})\,H(\gamma\gamma)$, $\lambda_{3H}=6$	11.03	7.91	3.12	0.39
$H(b\bar{b})\,H(\gamma\gamma)$, $\lambda_{3H}=10$	57.46	41.94	15.52	0.37
$gg\,H(\gamma\gamma)$	6.60	4.50	2.10	0.47
$t\bar{t}\,H(\gamma\gamma)$	13.21	9.82	3.39	0.35
$Z\,H(\gamma\gamma)$	3.62	2.44	1.18	0.48
$b\bar{b}\,H(\gamma\gamma)$	0.15	0.11	0.04	0.40
$b\bar{b}\gamma\gamma$	18.86	11.15	7.71	0.69
$c\bar{c}\gamma\gamma$	7.53	4.79	2.74	0.57
$jj\gamma\gamma$	3.34	1.59	1.75	1.10
$b\bar{b}j\gamma$	18.77	10.40	8.37	0.80
$c\bar{c}j\gamma$	5.52	3.94	1.58	0.40
$b\bar{b}jj$	5.54	3.81	1.73	0.45
$Z(b\bar{b})\gamma\gamma$	0.90	0.54	0.36	0.67
$t\bar{t}$ (≥ 1 leptons)	4.98	3.04	1.94	0.64
$t\bar{t}\gamma$ (≥ 1 leptons)	3.61	2.29	1.32	0.58
Total Background	92.63	58.42	34.21	0.59
Significance Z	1.163	1.090	0.487	
Combined significance		1.194		

1.194

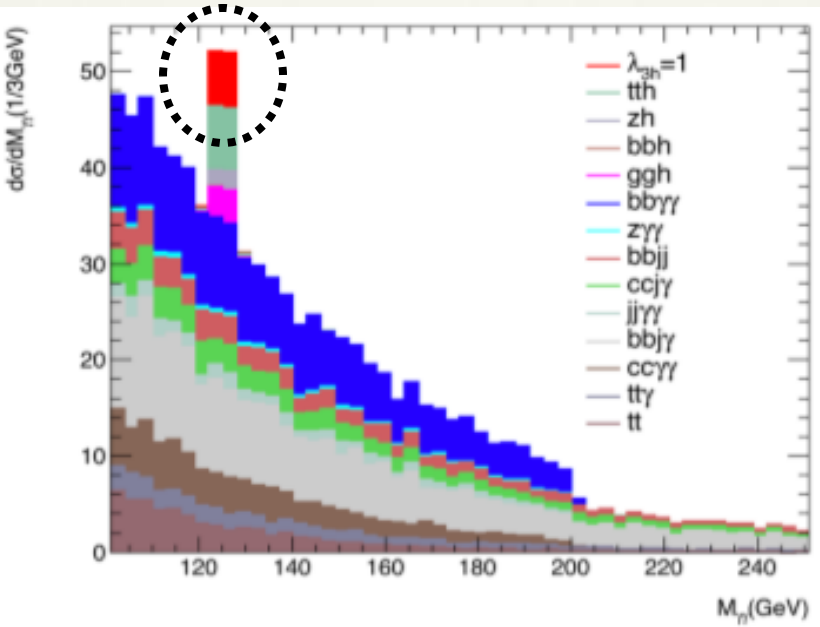

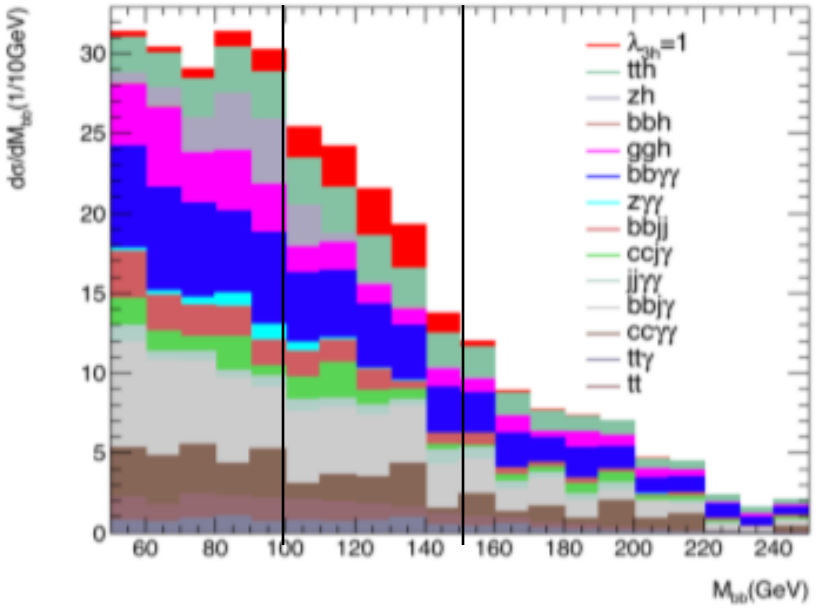

Essence of analysis results at the HL-LHC

$$Z = \sqrt{2 \cdot [((s+b) \cdot \ln(1+s/b) - s)]}$$

where s and b represent the numbers of signal and background events, respectively.

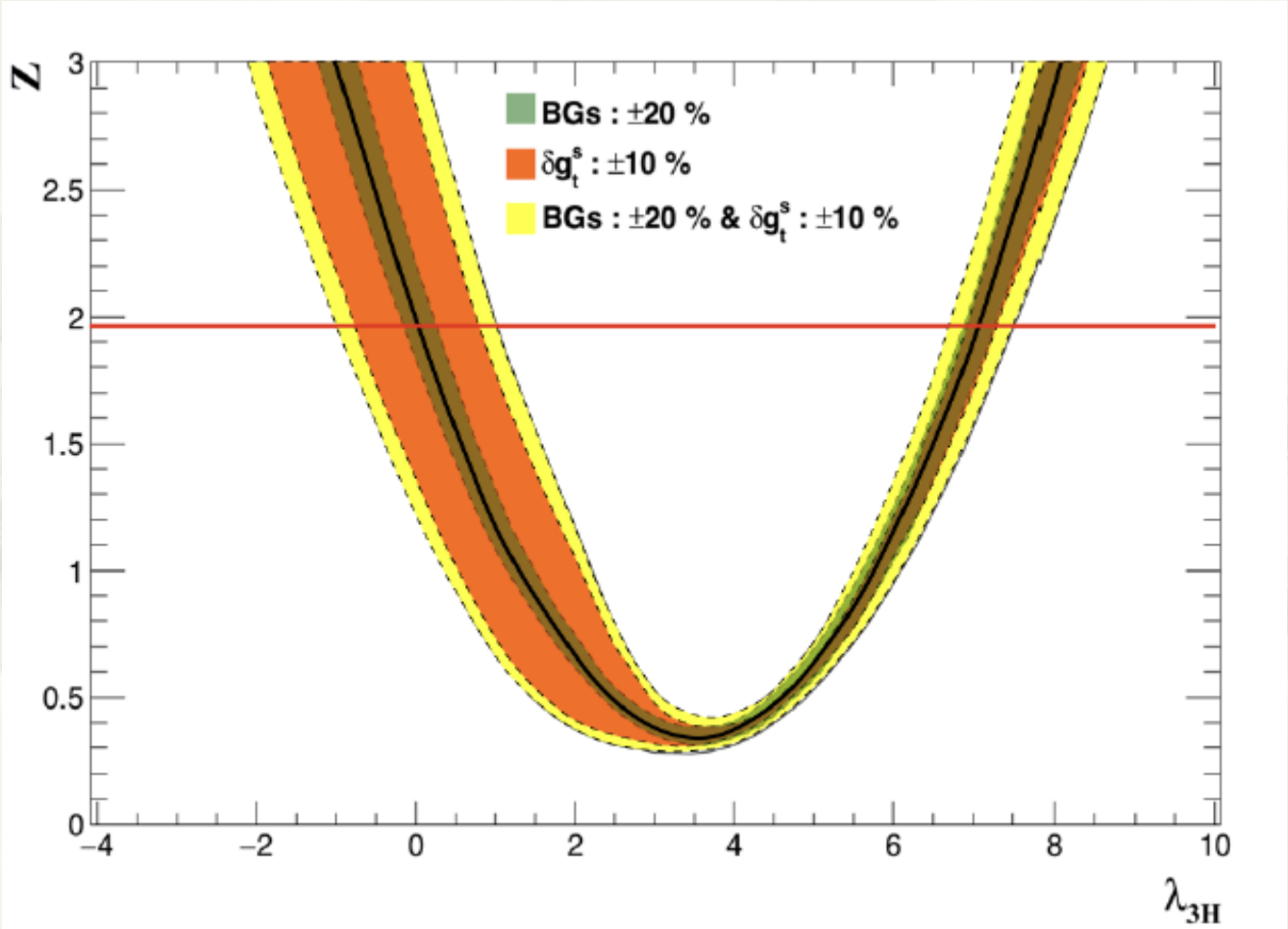

Essence of analysis results at the HL-LHC

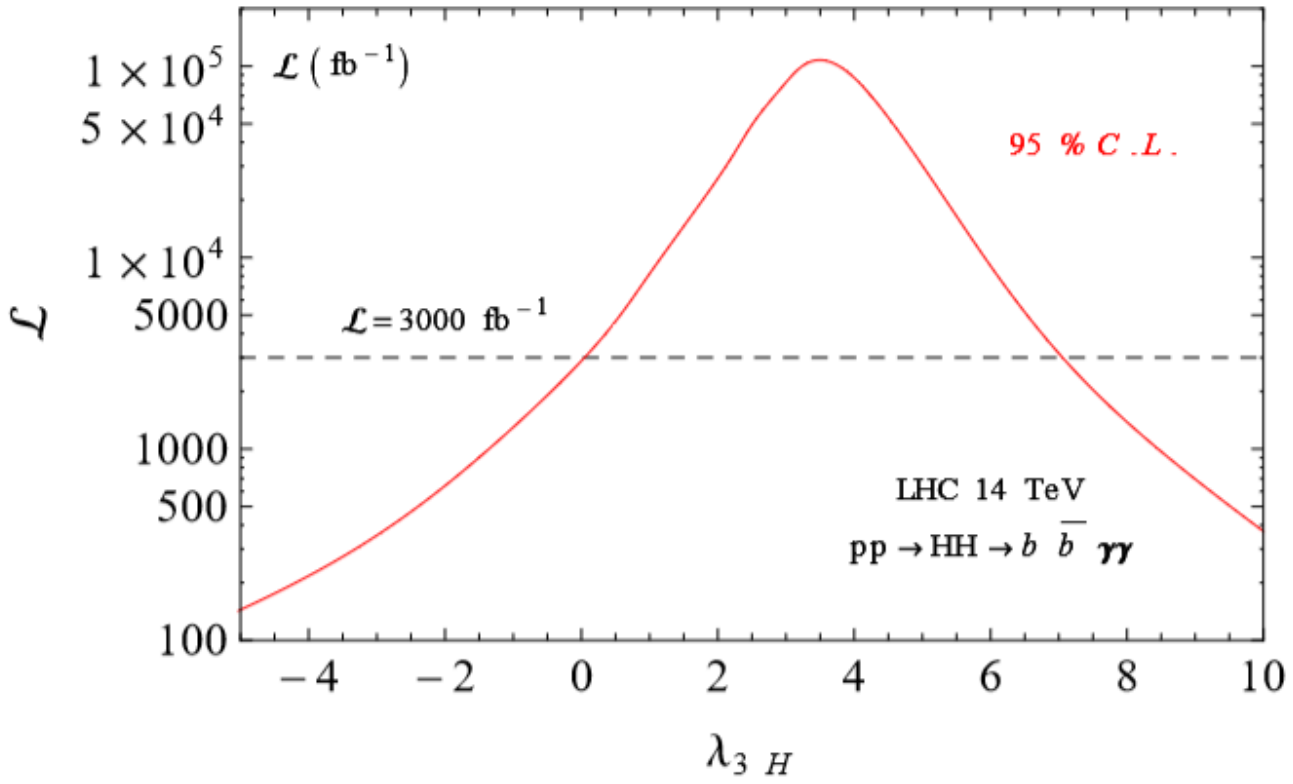

FIG. 7. **HL-LHC**: Required luminosity for 95% CL sensitivity at the 14 TeV HL-LHC versus λ_{3H}. Here we assume that the top-Yukawa coupling takes the SM value.

TABLE VII. The same as in Table I but for a 100 TeV hadron collider. In the row for $b\bar{b}H(\to\gamma\gamma)$, 5FS stands for the 5-flavor scheme.

Signal					
Signal process		Generator/Parton Shower	$\sigma \cdot BR$ [fb]	Order in QCD	PDF used
$gg \to HH \to b\bar{b}\gamma\gamma$ [16]		MG5_aMC@NLO/PYTHIA8	4.62	NNLO +NNLL	NNPDF2.3LO

Backgrounds					
Background(BG)	Process	Generator/Parton Shower	$\sigma \cdot BR$ [fb]	Order in QCD	PDF used
Single-Higgs associated BG	$ggH(\to\gamma\gamma)$ [16]	POWHEG − BOX/PYTHIA8	1.82×10^3	NNNLO	CT10
	$t\bar{t}H(\to\gamma\gamma)$ [16]	PYTHIA8/PYTHIA8	7.29×10^1	NLO	
	$ZH(\to\gamma\gamma)$ [16]	PYTHIA8/PYTHIA8	2.54×10^1	NNLO	
	$b\bar{b}H(\to\gamma\gamma)$ [30]	PYTHIA8/PYTHIA8	1.96×10^1	NNLO(5FS)	
Non-resonant BG	$b\bar{b}\gamma\gamma$	MG5_aMC@NLO/PYTHIA8	4.93×10^3	LO	CTEQ6L1
	$c\bar{c}\gamma\gamma$	MG5_aMC@NLO/PYTHIA8	4.54×10^4	LO	
	$jj\gamma\gamma$	MG5_aMC@NLO/PYTHIA8	5.38×10^5	LO	
	$b\bar{b}j\gamma$	MG5_aMC@NLO/PYTHIA8	1.44×10^7	LO	
	$c\bar{c}j\gamma$	MG5_aMC@NLO/PYTHIA8	4.20×10^7	LO	
	$b\bar{b}jj$	MG5_aMC@NLO/PYTHIA8	1.60×10^{10}	LO	
	$Z(\to b\bar{b})\gamma\gamma$	MG5_aMC@NLO/PYTHIA8	9.53×10^1	LO	
$t\bar{t}$ and $t\bar{t}\gamma$ BG [16] (≥ 1 lepton)	$t\bar{t}$	MG5_aMC@NLO/PYTHIA8	1.76×10^7	NLO	CT10
	$t\bar{t}\gamma$	MG5_aMC@NLO/PYTHIA8	4.18×10^4	NLO	CTEQ6L1

100TeV hadron collider

TABLE IX. The main fake processes and the corresponding faking rates in each sample of non-resonant and $t\bar{t}(\gamma)$ backgrounds. We recall that $P_{j\to\gamma} = 1.35 \times 10^{-3}$, $P_{c\to b} = P_{c_s\to b} = 0.1$ [16] and $P_{e\to\gamma} = 2\%/5\%$ in the barrel/endcap calorimeter region.

Background(BG)	Process	Fake Process	Fake rate
Non-resonant BG	$b\bar{b}\gamma\gamma$	N/A	N/A
	$c\bar{c}\gamma\gamma$	$c \to b$, $\bar{c} \to \bar{b}$	$(0.1)^2$
	$jj\gamma\gamma$	$c_s \to b$, $\bar{c}_s \to \bar{b}$	$(0.1)^2$
	$b\bar{b}j\gamma$	$j \to \gamma$	1.35×10^{-3}
	$c\bar{c}j\gamma$	$c \to b$, $\bar{c} \to \bar{b}$, $j \to \gamma$	$(0.1)^2 \cdot (1.35 \times 10^{-3})$
	$b\bar{b}jj$	$j \to \gamma$, $j \to \gamma$	$(1.35 \times 10^{-3})^2$
	$Z(\to b\bar{b})\gamma\gamma$	N/A	N/A
$t\bar{t}$	Leptonic decay	$e \to \gamma$, $e \to \gamma$	$(0.02)^2/0.02 \cdot 0.05/(0.05)^2$
	Semi-leptonic decay	$e \to \gamma$, $j \to \gamma$	$(0.02) \cdot 1.35 \times 10^{-3}/(0.05) \cdot 1.35 \times 10^{-3}$
$t\bar{t}\gamma$	Leptonic decay	$e \to \gamma$	0.02/0.05
	Semi-leptonic	$e \to \gamma$	0.02/0.05

Outline of simulations and event selections

TABLE X. Sequence of event selection criteria at the HL-100 TeV hadron collider applied in this analysis.

Sequence	Event Selection Criteria at the HL-100 TeV hadron collider
1	Di-photon trigger condition, ≥ 2 isolated photons with $P_T > 30$ GeV, $\|\eta\| < 5$
2	≥ 2 isolated photons with $P_T > 40$ GeV, $\|\eta\| < 3$, $\Delta R_{j\gamma} > 0.4$
3	≥ 2 jets identified as b-jets with leading(subleading) $P_T > 50(40)$ GeV, $\|\eta\| < 3$
4	Events are required to contain ≤ 5 jets with $P_T > 40$ GeV within $\|\eta\| < 5$
5	No isolated leptons with $P_T > 40$ GeV, $\|\eta\| < 3$
6	$0.4 < \Delta R_{b\bar{b}} < 3.0$, $0.4 < \Delta R_{\gamma\gamma} < 3.0$
7	$122.5 < M_{\gamma\gamma}/\text{GeV} < 127.5$ and $90 < M_{b\bar{b}}/\text{GeV} < 150$
8	$P_T^{\gamma\gamma} > 100$ GeV, $P_T^{b\bar{b}} > 100$ GeV

TABLE XII. The same as in Table VI but at the HL-100 TeV hadron collider with an integrated luminosity of 3 ab^{-1}.

Expected yields (3000 fb^{-1}) Samples	Total	Barrel-barrel	Other (End-cap)	Ratio (O/B)
$H(b\bar{b})\,H(\gamma\gamma)$, $\lambda_{3H}=-4$	5604.46	4257.36	1347.10	0.32
$H(b\bar{b})\,H(\gamma\gamma)$, $\lambda_{3H}=0$	1513.56	1163.04	350.52	0.30
$H(b\bar{b})\,H(\gamma\gamma)$, $\lambda_{3H}=1$	941.37	723.86	217.51	0.30
$H(b\bar{b})\,H(\gamma\gamma)$, $\lambda_{3H}=2$	557.36	431.45	125.91	0.29
$H(b\bar{b})\,H(\gamma\gamma)$, $\lambda_{3H}=6$	753.18	566.18	187.00	0.33
$H(b\bar{b})\,H(\gamma\gamma)$, $\lambda_{3H}=10$	3838.33	2924.25	914.08	0.31
$gg\,H(\gamma\gamma)$	890.47	742.97	147.50	0.20
$t\bar{t}\,H(\gamma\gamma)$	868.73	659.33	209.40	0.32
$Z\,H(\gamma\gamma)$	168.86	122.91	45.95	0.37
$b\bar{b}\,H(\gamma\gamma)$	9.82	7.00	2.82	0.40
$b\bar{b}\gamma\gamma$	783.87	443.70	340.17	0.77
$c\bar{c}\gamma\gamma$	222.88	111.44	111.44	1.00
$jj\gamma\gamma$	32.28	20.98	11.30	0.54
$b\bar{b}j\gamma$	1982.88	1516.32	466.56	0.31
$c\bar{c}j\gamma$	293.81	216.49	77.32	0.36
$b\bar{b}jj$	3674.16	1924.56	1749.60	0.91
$Z(b\bar{b})\,\gamma\gamma$	54.87	35.72	19.15	0.54
$t\bar{t}$ (≥ 1 leptons)	59.32	38.32	21.00	0.55
$t\bar{t}\gamma$ (≥ 1 leptons)	105.68	62.53	43.15	0.69
Total Background	9147.63	5902.37	3245.36	0.55
Significance Z	9.681	9.239	3.777	
Combined significance		9.981		

9.981

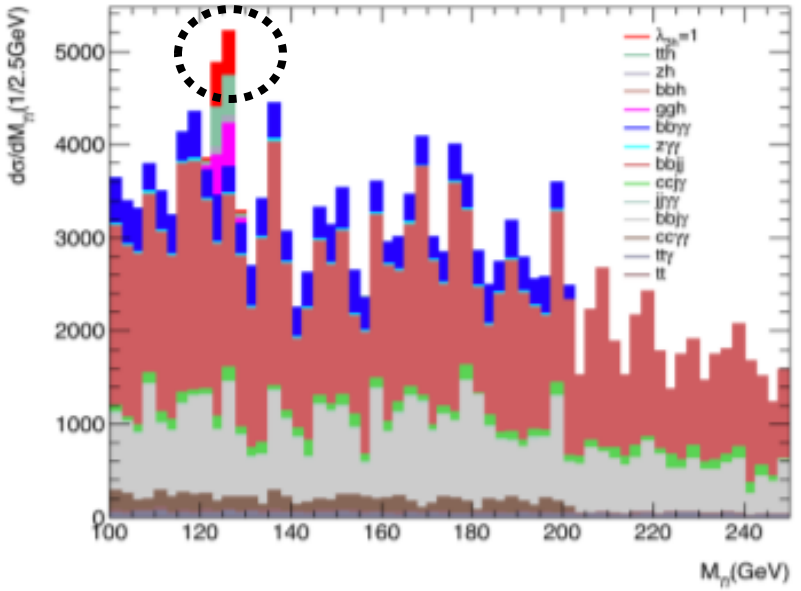

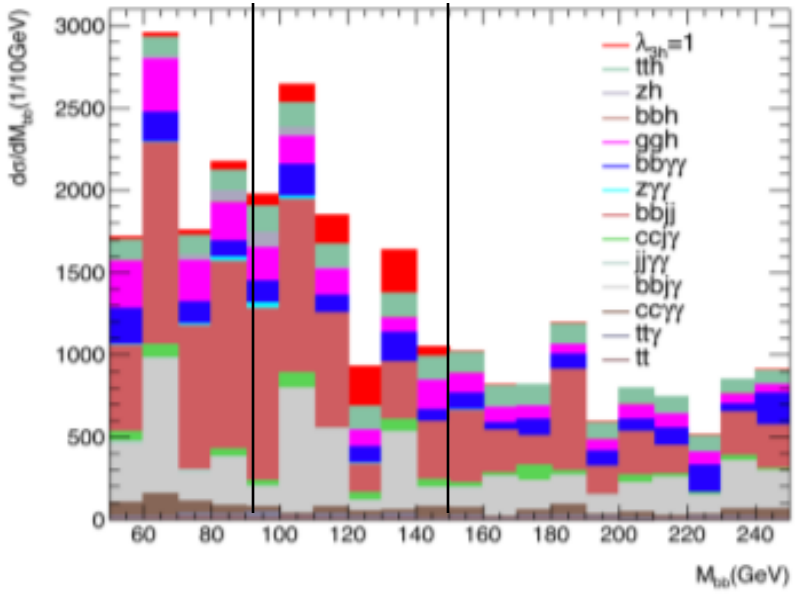

Essence of analysis results at the HL-100 TeV hadron collider

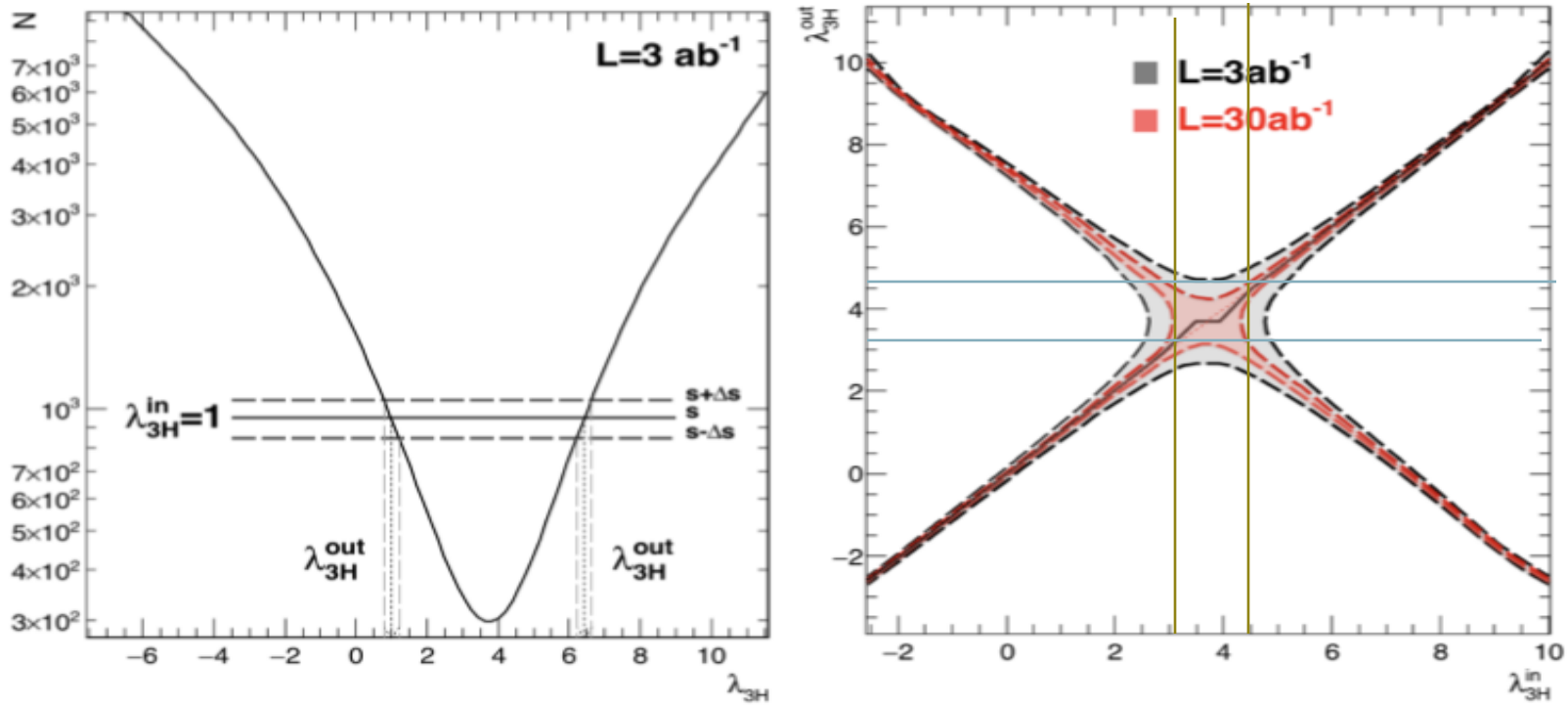

FIG. 9. **HL-100 TeV**: (Left) The number of signal events N versus λ_{3H} with 3 ab^{-1}. The horizontal solid line is for the number of signal events s when $\lambda_{3H}^{\rm in} = 1$ and the dashed lines for $s \pm \Delta s$ with the statistical error of $\Delta s = \sqrt{s+b}$. (Right) The 1-σ error regions versus the input values of $\lambda_{3H}^{\rm in}$ assuming 3 ab^{-1} (black) and 30 ab^{-1} (red).

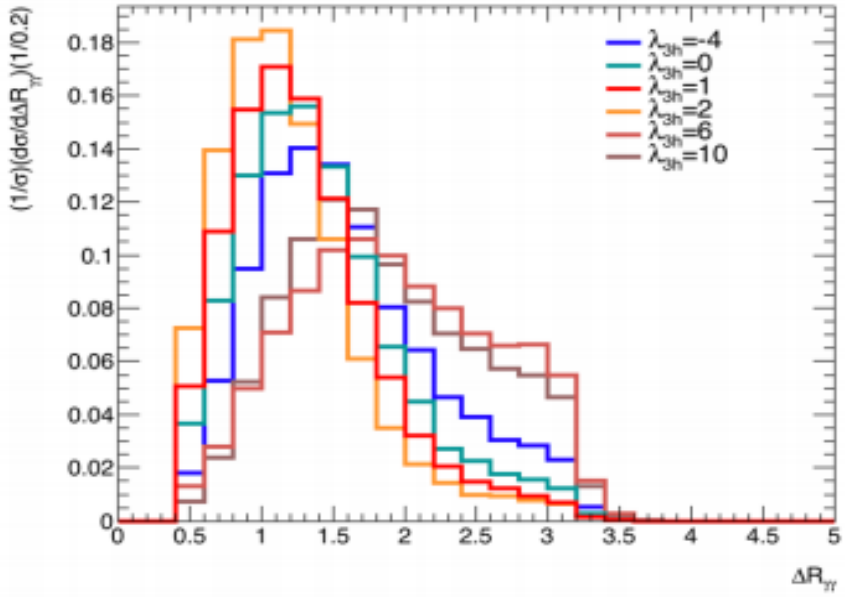

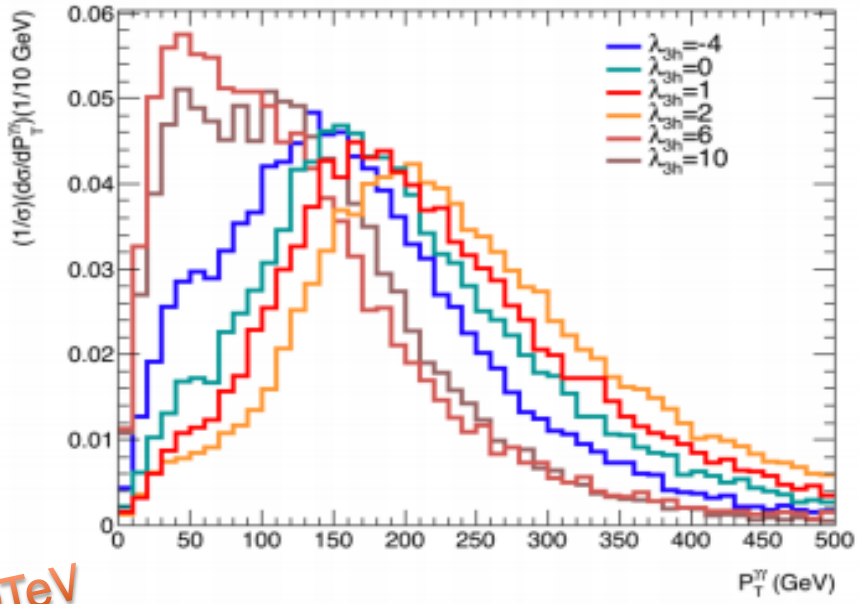

100TeV
hadron collider

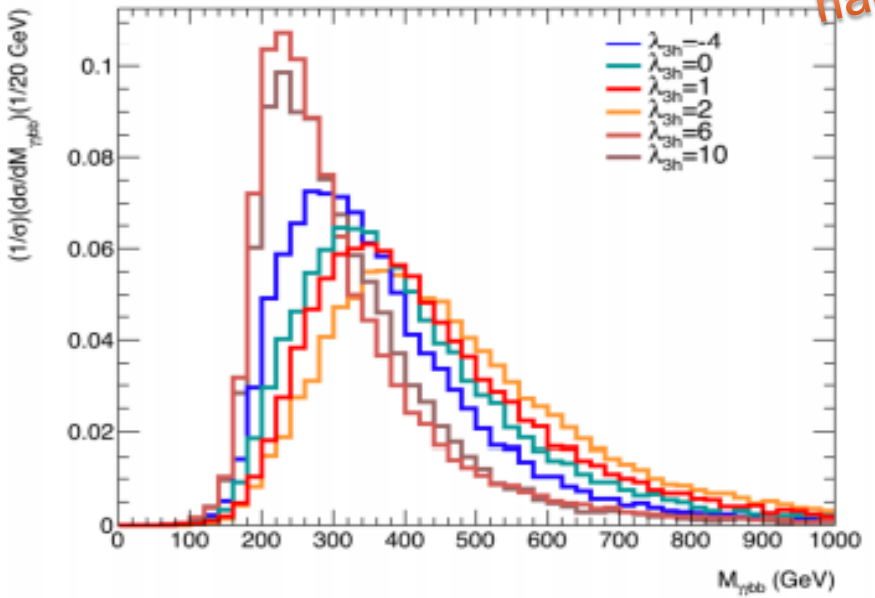

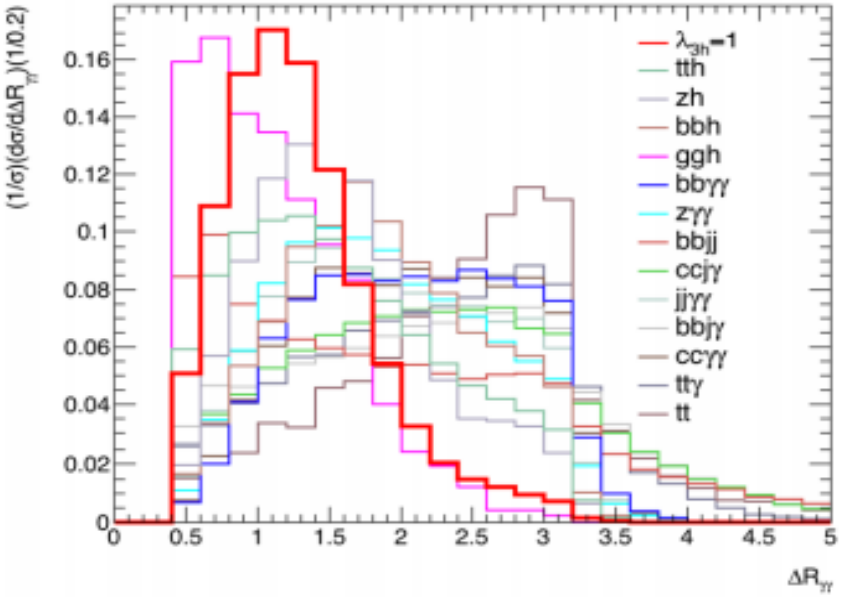

Essence of analysis results at the HL-100 TeV hadron collider

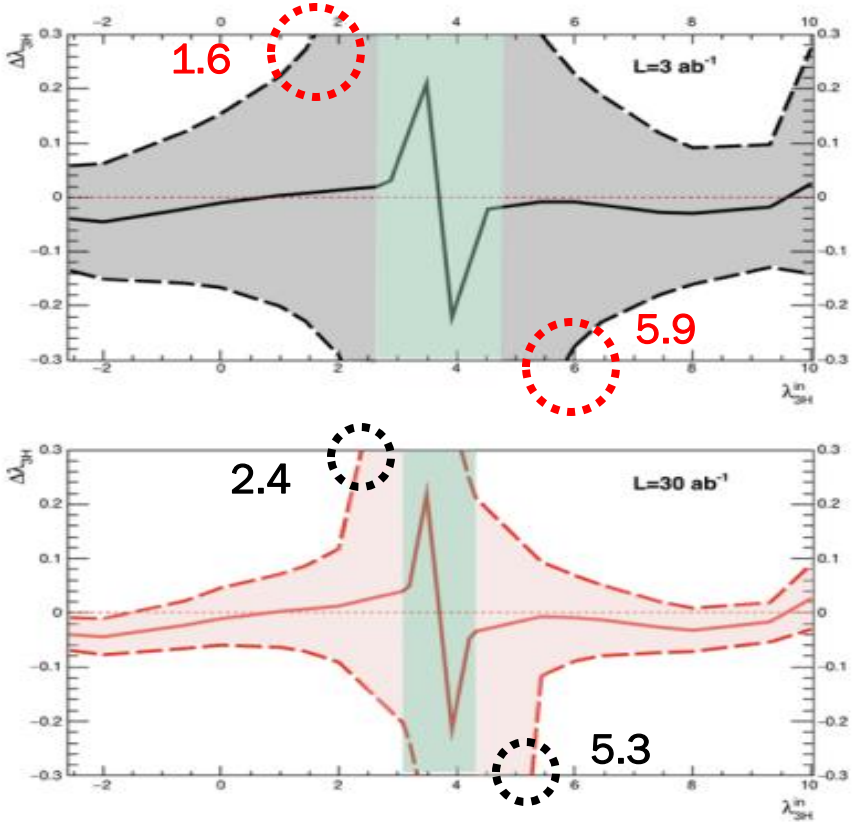

FIG. 10. **HL-100 TeV**: $\Delta\lambda_{3H} = \lambda_{3H}^{\rm out} - \lambda_{3H}^{\rm in}$ versus $\lambda_{3H}^{\rm in}$ along the $\lambda_{3H}^{\rm out} = \lambda_{3H}^{\rm in}$ line with 3 ab^{-1} (upper) and 30 ab^{-1} (lower). The lines are the same as in the right frame of Fig. 9. We consider $|\Delta\lambda_{3H}| \leq 0.3$ to find the regions in which one can pin down the λ_{3H} coupling with an absolute error smaller than 0.3.

Conclusions [HL-LHC]

- We find that even for the most promising channel $HH \to b\bar{b}\gamma\gamma$ at the HL-LHC with a luminosity of $3000\ \text{fb}^{-1}$, the significance is still not high enough to establish the Higgs self-coupling at the SM value.
- Instead, we can only constrain the self-coupling to $-1.0 < \lambda_{3H} < 7.6$ at 95% confidence level after considering the uncertainties associated with the top-Yukawa coupling and the estimation of backgrounds.

Conclusions [HL-100 TeV hadron collider]

- With a luminosity of $3\ \mathrm{ab}^{-1}$, we find there exists a bulk region of $2.6 \lesssim \lambda_{3H} \lesssim 4.8$ in which one can't pin down the trilinear coupling.
- At the SM value, we show that the coupling can be measured with about 20% accuracy.
- While assuming $30\ \mathrm{ab}^{-1}$, the bulk region reduces to $3.1 \lesssim \lambda_{3H} \lesssim 4.3$ and the trilinear coupling can be measured with about 7% accuracy at the SM value.